PROCEEDINGS OF SPIE

SPIEDigitalLibrary.org/conference-proceedings-of-spie

Low-cost high-performance W-band LNA MMICs for millimeter-wave imaging

Michael G. Case, Carl W. Pobanz, Sander Weinreb, Mehran Matloubian, Ming Hu, et al.

Michael G. Case, Carl W. Pobanz, Sander Weinreb, Mehran Matloubian, Ming Hu, Michael Wetzel, Paul Janke, Catherine M. H. Ngo, "Low-cost high-performance W-band LNA MMICs for millimeter-wave imaging," Proc. SPIE 4032, Passive Millimeter-Wave Imaging Technology IV, (20 July 2000); doi: 10.1117/12.391824

SPIE.

Event: AeroSense 2000, 2000, Orlando, FL, United States

Downloaded From: https://www.spiedigitallibrary.org/conference-proceedings-of-spie on 7/31/2018 Terms of Use: https://www.spiedigitallibrary.org/terms-of-use

Low-Cost, High-Performance W-Band LNA MMICs for Millimeter-Wave Imaging

Michael G. Case, Carl Pobanz, Sander Weinreb*, Mehran Matloubian,
Ming Hu, Michael Wetzel, Paul Janke, and Catherine Ngo

HRL Laboratories LLC, 3011 Malibu Canyon Road, Malibu, California 90265

*JPL, 4800 Oak Grove Drive, Pasadena, California 91109

ABSTRACT

The main limitation to the sensitivity of a radiometer or imager is its equivalent noise temperature, T_e. Placing a low noise amplifier (LNA) at a radiometer's front end can dramatically reduce T_e. LNA performance has steadily improved over recent years, and here we report on a W-band LNA with the lowest T_e measured at room temperature. Furthermore, we present statistical RF data showing high yield and consistency for future high volume production that is needed for commercial radiometric imaging array applications such as security screening, aircraft landing, and other systems.

Previously, the lowest noise room temperature (290 K) W-band LNA demonstrated 3.3 dB noise figure (NF) (T_e = 330 K) with 20 dB associated gain[1], although the average NF was 4.4 dB (T_e > 500 K) over the 92 to 96 GHz band. Here we present measurements of an InP-based 0.1 μm HEMT 4-stage LNA MMIC (86LN3) with an average NF of 2.5 dB (T_e = 225 K) and average gain of 30 dB over a 76 to 96 GHz band. This is the lowest reported room temperature LNA noise figure to the authors' knowledge, and demonstrates the performance capability of this HEMT technology. Two other, more conservative designs (70LN3A and 86LN1A) were chosen for higher-volume production with 24 dB gain, 3.2 dB NF (T_e = 315 K) and 21 dB gain, 2.9 dB NF (T_e = 275 K) respectively at the center of the band, 85 GHz. These LNAs were fabricated on 3" wafers containing 1700 die with an average DC yield of 70% and 98% of DC good die passing RF screening.

Keywords: InP, MMIC, W-band, Millimeter-Wave, Low-Noise Amplifier (LNA)

1. INTRODUCTION

Millimeter waves penetrate many materials that are opaque to visible and IR light, enabling high-resolution imaging of scenes that were previously invisible. Examples include weapons concealed beneath clothing or a runway obscured by fog. The emissivity range of objects at millimeter wavelengths is very large, 10 times greater than in the infrared, so high contrast images can be made using naturally existing blackbody radiation. Creating such an image has been historically difficult due to the lack of small, sensitive millimeter-wave detectors that could easily be arrayed. Cameras relied on a single detector element or small array in conjunction with a mechanically scanned mirror to cover a scene in several minutes time. Recent developments in low-noise InP HEMT technology make it possible to amplify directly the millimeter-wave radiation at each pixel in a focal plane and rectify these signals to form images at full-motion frame rates.

The purpose of the millimeter-wave imaging system is to detect the spatially distributed radiation emitted by an object in view. This is done at each pixel by a radiometer, which comprises a low-noise amplifier (LNA) whose input is switched between the radiation from the scene and that from a resistor at a reference temperature. The difference in millimeter-wave power at the output of the LNA between these two states is detected to yield the effective temperature of the area in view. The time it takes to produce a thermal radiation image depends ultimately on the number of detectors operating in parallel, and the integration time τ required by each detector to measure temperature T_{scene} with an uncertainty ΔT. High quality images typically require a ΔT resolution of at least 0.5 K, and higher resolution is especially desired for indoor applications

- Mgcase@hrl.com, phone: (310) 317-5793, FAX: (310) 317-5450
- *72164.560@compuserve.com (818) 354-4065

Downloaded From: https://www.spiedigitallibrary.org/conference-proceedings-of-spie on 7/31/2018
Terms of Use: https://www.spiedigitallibrary.org/terms-of-use

like security screening. Using a receiver with a wide bandwidth (B) and low noise (T_{sys}) minimizes integration time, according to the radiometer law:

$$\Delta T = \frac{T_{sys} + T_{scene}}{\sqrt{B\tau}}. \quad (1)$$

2. InP-BASED HEMT DEVICE TECHNOLOGY

InP HEMT devices provide higher gain and lower noise at higher operating frequencies as compared to other solid state devices such as GaAs-based PHEMTs. These benefits are due to the superior electron mobility and velocity in the high-indium-content GaInAs channel, along with increased carrier density in the channel due to the large conduction band discontinuity at the AlInAs/GaInAs heterojunction[2,3]. The state-of-the-art in both mm-wave amplifiers and LNAs has been set using such devices. The advanced HRL HEMT device has demonstrated a substantial improvement in mm-wave and sub-mm-wave amplifier performance. Previously, a 3-stage amplifier with a peak gain of 12 dB at 155 GHz[4] set the record at 4 dB per stage at D-band frequencies. A recent demonstration of a single stage amplifier with a peak gain of 10 dB at 140 GHz[5] (10 dB per stage) using the HRL HEMT has increased this benchmark. The highest performance W-band LNA reported to date was a 3-stage amplifier with 4.4 dB average NF (3.3 dB minimum) and 20 dB associated gain over the 92 to 96 GHz band[1]. The work reported here on a 4-stage LNA using the HRL HEMT achieves an average NF of 2.5 dB and an average gain of 30 dB over the 76 to 96 GHz band.

$Ga_{0.47}In_{0.53}As$	CAP	DOPED
$Al_{0.48}In_{0.52}As$	SCHOTTKY	UNDOPED
$Al_{0.48}In_{0.52}As$	DONOR	Si-DOPED
$Al_{0.48}In_{0.52}As$	SPACER	UNDOPED
$Ga_{0.20}In_{0.80}As$	CHANNEL	UNDOPED
InP	CHANNEL	UNDOPED
InP	CHANNEL	Si-DOPED
$Al_{0.48}In_{0.52}As$	BUFFER	UNDOPED
InP	SUBSTRATE	

Figure 1. Device channel profile for the 0.1 µm InAlAs/GaInAs/InP HEMT.

The MMICs are fabricated in a 0.1 µm AlInAs/GaInAs/InP HEMT technology with the material structure shown in Fig. 1. It consists of a high-indium content $Ga_{0.20}In_{0.80}As$ channel and a high resistivity buffer layer for reducing the output conductance of the device. This results in HEMTs with both high f_T and f_{MAX} values. Boron ion implantation is used for device isolation resulting in a fully planar process. Source and drain ohmic contacts are formed with AuGe/Ni/Au alloy having a typical contact resistance of 0.1 Ω-mm. The gates have a T-cross section with a length of 0.1 µm at the semiconductor interface, and are formed using Ti/Pt/Au lift-off. Transmission lines and other interconnections are formed using a thicker (1.5 µm) Ti/Pt/Au lift-off process. The devices are passivated with a 500Å layer of PECVD Si_3N_4. Additional components for MMICs are electro-plated airbridges, MIM capacitors with 1000Å PECVD Si_3N_4, and epitaxial resistors having a sheet resistance of 160 Ω/□. After complete front-side processing, the wafer is thinned to 50 µm then via holes are wet etched and plated with gold.

The devices exhibit a DC transconductance (g_m) of 950 mS/mm with a full channel current of 700 mA/mm and gate-drain breakdown voltage of 5V. The measured RF transconductance is greater than 1100 mS/mm with an extrinsic current gain cutoff frequency (f_T) exceeding 250 GHz. The 150 µm HEMT used for characterization has four gate fingers of 37.5 µm width each, and is laid out in a CPW configuration with the source pads connected by airbridges.

Figure 2 is a plot of the maximum stable gain (MSG) and the 50 Ω transducer gain $|S_{21}|^2$ vs. frequency for a 150 µm device biased at V_{ds} = 1.5 V and I_{ds} = 56 mA. These measurements were performed on-wafer in a continuous sweep from 2-110 GHz

Downloaded From: https://www.spiedigitallibrary.org/conference-proceedings-of-spie on 7/31/2018
Terms of Use: https://www.spiedigitallibrary.org/terms-of-use

using an HP 8510XF network analyzer with 1.0 mm coaxial wafer probes, calibrated by the line-reflect-match (LRM) method. An MSG of 14 dB was measured at the instrumentation limit of 110 GHz, where the device is still potentially unstable ($K<1$). Extrapolating the gain at -6 dB per octave from this point indicates a maximum frequency of operation (f_{MAX}) of approximately 600 GHz. Although HEMT gain extrapolation is complicated by potential gain resonance phenomena as f_{MAX} is approached, this figure of merit is supported by a measured MMIC gain of 10 dB per stage at 140 GHz[5].

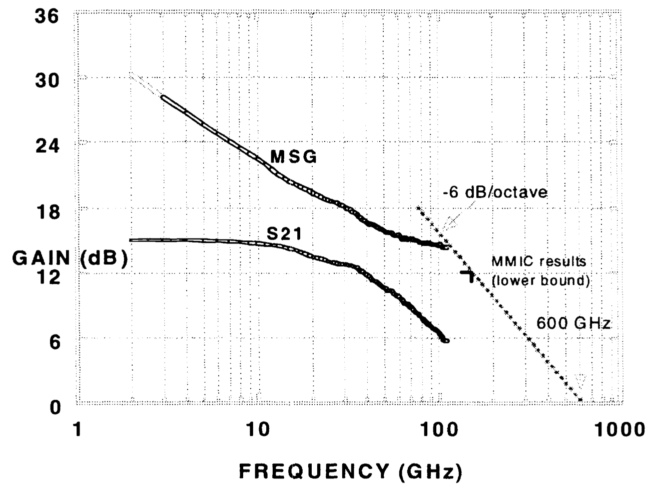

Figure 2. Gain of 150 μm HEMT from 2-110 GHz at V_{ds}=1.5V, I_{ds}=56 mA. Calibrated on-wafer measurement using HP8510XF network analyzer with 1.0-mm coaxial probes.

Noise parameters for the HEMTs were extracted between 2 to 40 GHz, and by combining them with broadband S-parameter measurements, an equivalent circuit model was developed. This model employs the Pospieszalski technique of elevating the temperature of the drain-source conductance to simultaneously match the scattering and noise data without the need for correlated noise sources[6]. The equivalent drain temperature (T_D) for these transistors is typically 1500 K.

3. LOW-NOISE AMPLIFIER CIRCUIT DESIGN

Several LNAs were designed into the process using both coplanar waveguide (CPW) and microstrip transmission line environments. The CPW approach provides lower inductance connections to the transistor's source and allows DC testing before backside processing, but more care must be taken with discontinuities and high-order modes than for microstrip circuits. Using backside vias placed roughly $\lambda/4$ apart suppresses undesirable modes in the CPW. Since the transistors have such a high f_{MAX}, amplifier stability and excessive gain both below and above the band of interest were important design considerations. Another significant design constraint was a maximum die size set by final packaging. The MMICs will ultimately be placed within a waveguide cavity that is cutoff for W-band signals, preventing the mm-wave energy in the quasi-TEM mode transmission lines from radiating into the package. Accounting for other adjacent components and fixture requirements set the maximum die width to 790 μm. Furthermore, to allow interchangeability, all amplifiers were forced to the same length, 2 mm, resulting in a total die area of 1.6 mm^2.

The RF performance goals were > 10 dB return loss and > 20 dB gain with the lowest noise figure possible. The minimum noise figure should be 1.6 dB for the device alone at 95 GHz based the equivalent circuit model. But, since the device is only conditionally stable (K=0.6) at 95 GHz, lossy matching networks and feedback were employed to stabilize the amplifier at the expense of performance. The CPW circuit (Fig. 3) was designed using band-pass tuning networks, while the microstrip variation (Fig. 4) used low-pass. As mentioned earlier, the CPW circuit was designed more conservatively to meet module requirements over a larger process variation; the microstrip circuit provided a much smaller safety margin.

Downloaded From: https://www.spiedigitallibrary.org/conference-proceedings-of-spie on 7/31/2018
Terms of Use: https://www.spiedigitallibrary.org/terms-of-use

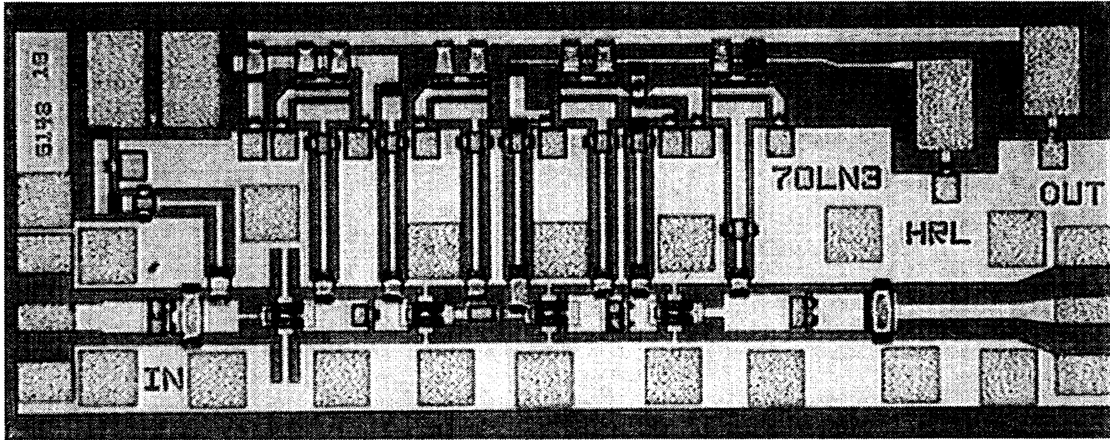

Figure 3. CPW LNA photograph. Band-pass tuning is evident as different sized series capacitors and transmission lines with shunt inductive stubs.

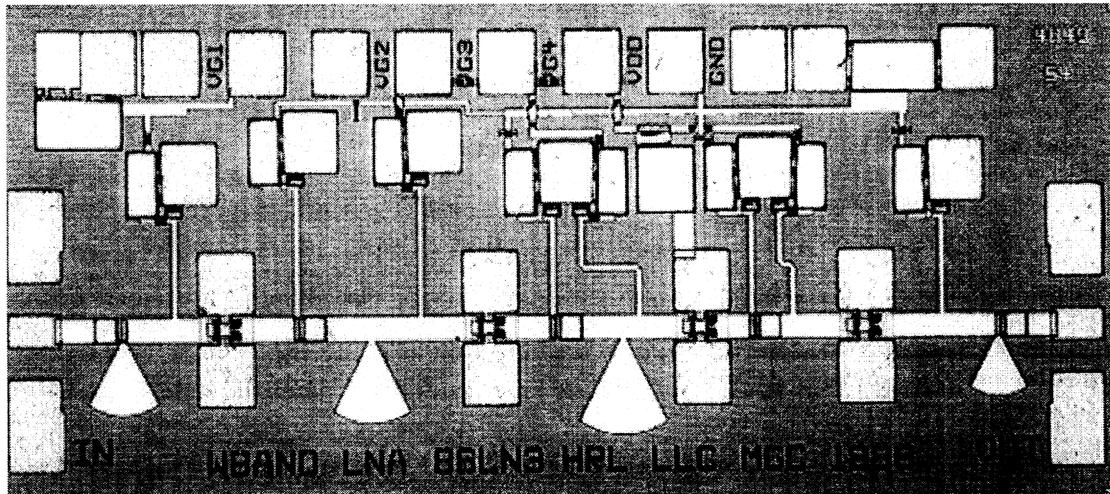

Figure 4. Microstrip LNA photograph. Low-pass tuning is evident as different series transmission line and shunt radial stub lengths.

The circuits were designed to accommodate troubleshooting and bias tuning. The drains of all the stages are connected in parallel. The gates are connected in parallel as well, but they have airbridges connecting them that can easily be broken to allow independent control for each stage. Significant amounts of decoupling resistor-capacitor networks are used on both the gate and drain bias lines to prevent low frequency oscillations and interactions while facilitating common bias application.

4. AMPLIFIER CHARACTERIZATION

All amplifiers were fully tested on-wafer immediately before dicing on a Cascade Summit 10,000 probe station with GGB Picoprobes for signal (WR-10 waveguide flange) and bias (needle probes with bypass networks). DC measurements verified functional amplifiers having sufficient maximum current, transconductance, breakdown voltage, and pinch-off leakage current using an HP 4145B. Scattering parameters were measured with a Wiltron 360B network analyzer with modified W-band transmit/receive modules, and 50 Ω noise figure and gain were measured using a custom Spacek Laboratories fundamental mixer connected to an HP 8970B noise figure meter and Millitech solid-state noise source. Several issues arose during RF testing that bear note.

Most commercial waveguide-based network analyzers provide a large stimulus signal, on the order of 10 mW. This enhances the signal-to-noise ratio (SNR) of the detected forward and reverse waves since the signal is large, but overdrives high-gain

Downloaded From: https://www.spiedigitallibrary.org/conference-proceedings-of-spie on 7/31/2018
Terms of Use: https://www.spiedigitallibrary.org/terms-of-use

active circuits and devices. Since the LNAs measured have a 1 dB gain compression between 1 and 10 mW output power (depending on bias conditions), the drive power had to be reduced substantially to obtain small-signal scattering matrices. Inserting attenuators at the external port of the mm-wave module would reduce the drive power, but the SNR of the transmitted signal would be degraded by that attenuation, and the reflected signal would be degraded by that attenuation doubled. Since we needed approximately 30 dB of attenuation, this technique proved terribly inaccurate. By placing the attenuator between the mm-wave source and the directional coupler within the mm-wave module, only single-pass attenuation degraded both forward and reverse wave signals. This modification was accomplished with little disruption of the module hardware. A much better solution would be to modify the directional couplers within the module to transmit from the weakly coupled port rather than the main line, but this would have required re-engineering the entire module.

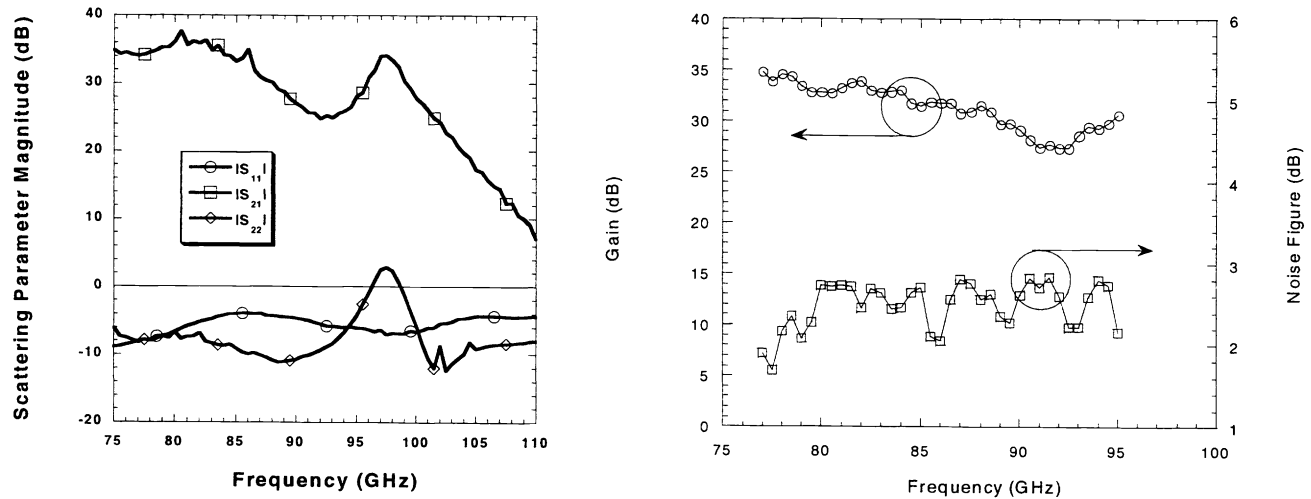

Figure 5. Measured scattering parameters (left) and gain and noise figure (right) of a microstrip LNA 86LN3. The return gain and insertion gain bump at 97 GHz proved too problematic (unstable) for use in an array. The CPW amplifiers had less significant gain flatness and stability problems.

Since the solid-state noise source emits such a small amount of power (approximately -174 dBm in the cold state, 10 to 20 dB higher in the hot state), amplifier saturation is not a significant issue and true small-signal gain is measured. What can be significant is the impedance mismatch of the noise source and or the down converter used to detect the signal especially as the impedance changes between the hot and cold states. Impedance mismatch typically shows up as periodicity in the gain and noise figure curves over frequency. An isolator cascaded with the noise source tremendously reduces mismatch issues at the input to the amplifier. Using an additional isolator before the receiver reduces system related artifacts even more. Impedance mismatch in a network analyzer is removed through routine calibration. In the measurements presented here, we use isolators at both source and receiver locations.

Since the noise figure meter uses the ratio between the hot and cold noise powers (excess noise ratio, ENR) to calculate the noise figure of the device under test, precise knowledge of that ratio is critical to accurate measurement. The Raytheon Primary Standards Laboratory calibrates our noise source with the isolator in place using the comparison method to the ENR of a noise tube calibrated by the National Institute of Standards with an estimated uncertainty of ± 0.4 dB. The measured ENR is then reduced by the insertion loss of the waveguide and probe used to contact the MMIC within the wafer. These losses were measured with the noise figure meter by calibrating to the known ENR reference plane than inserting the waveguide used at the input port and measuring the loss. The manufacturer measured the wafer probe loss. The sum of these losses was then compared to a symmetric arrangement using identical probes and waveguide at the input and output ports, and agreement was within 0.1 dB across the band.

Each and every amplifier was measured in the six-wafer lot. RF measurements were taken on all die passing DC requirements. A significant improvement to our measurement system would be using an electronic waveguide switch to sequentially measure the scattering parameters and noise figure with a single probe contact. Our current system required separate prober configurations for the two RF measurements. The highest gain and lowest noise were achieved with the

Downloaded From: https://www.spiedigitallibrary.org/conference-proceedings-of-spie on 7/31/2018
Terms of Use: https://www.spiedigitallibrary.org/terms-of-use

86LN3 microstrip LNA (Fig. 5). Two CPW LNA designs were chosen for the production run: 70LN3A (Fig. 6 and 7) with higher gain, and 86LN1A (Fig. 8 and 9) with lower noise. Statistics for all the measured amplifiers are given in Table 1.

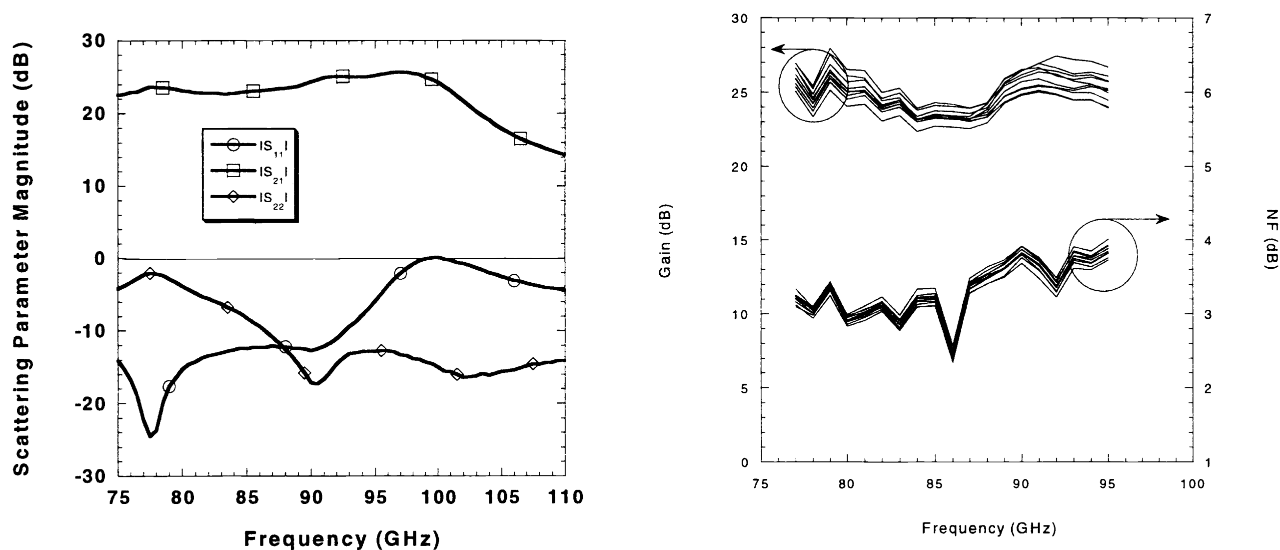

Figure 6. Measured scattering parameters for a single (left) and gain and noise figure for 10 (right) 70LN3A amplifiers from wafer # 1669.

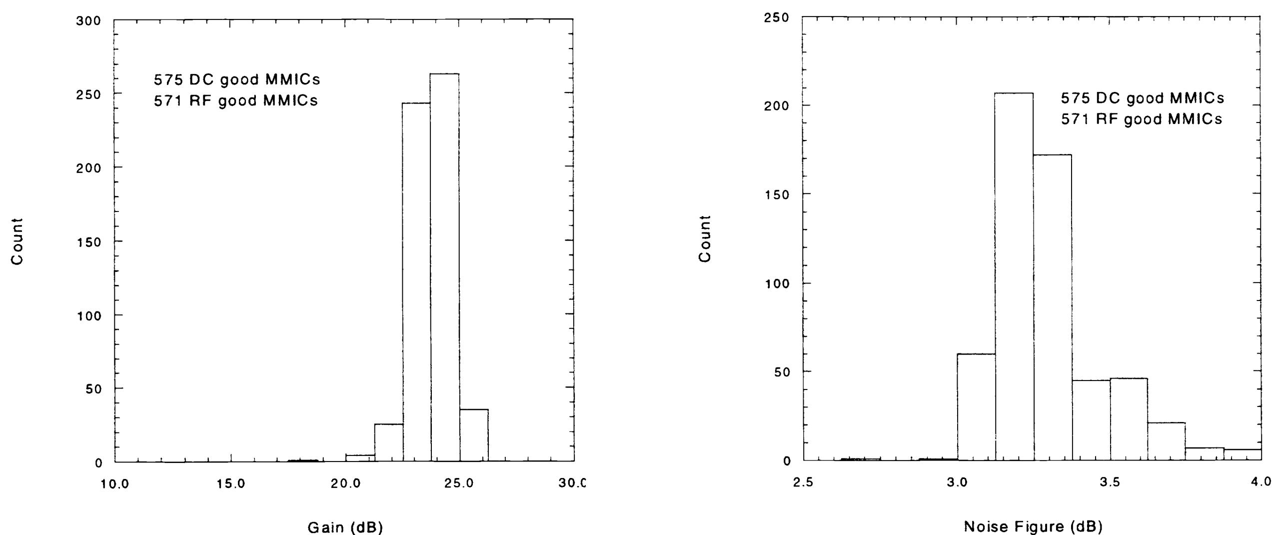

Figure 7. Histograms showing process consistency for gain (left) and noise figure (right) for the 70LN3A amplifiers at 85 GHz from wafer # 1669.

Downloaded From: https://www.spiedigitallibrary.org/conference-proceedings-of-spie on 7/31/2018
Terms of Use: https://www.spiedigitallibrary.org/terms-of-use

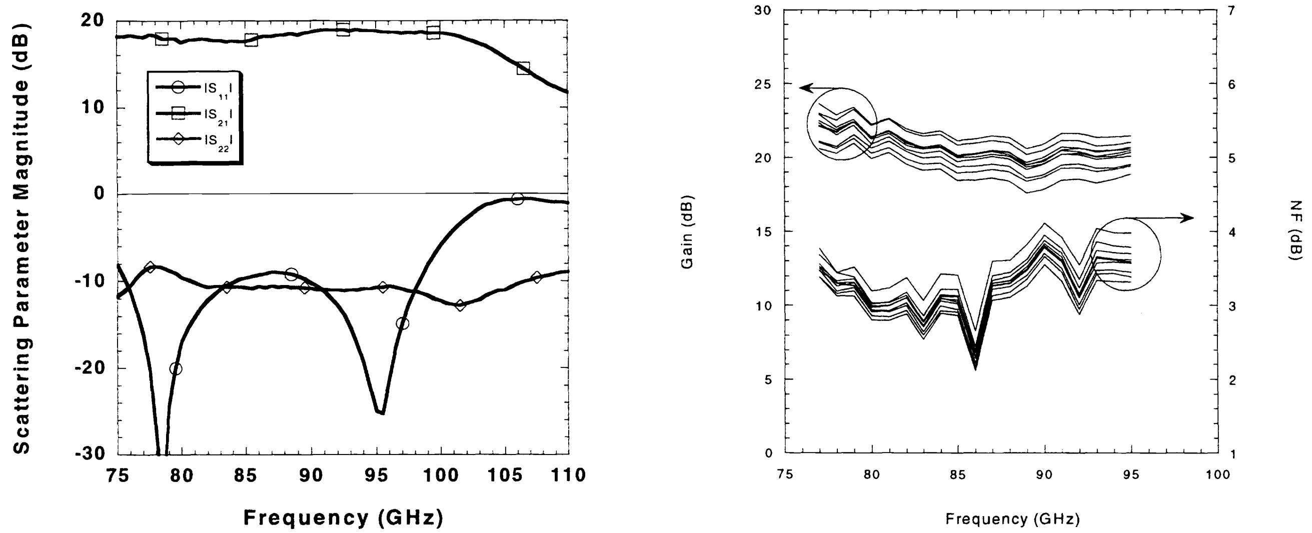

Figure 8. Measured scattering parameters for a single (left) and gain and noise figure for 10 (right) 86LN1A amplifiers from wafer # 1669. Excessive power from the network analyzer stimulus signal caused gain compression.

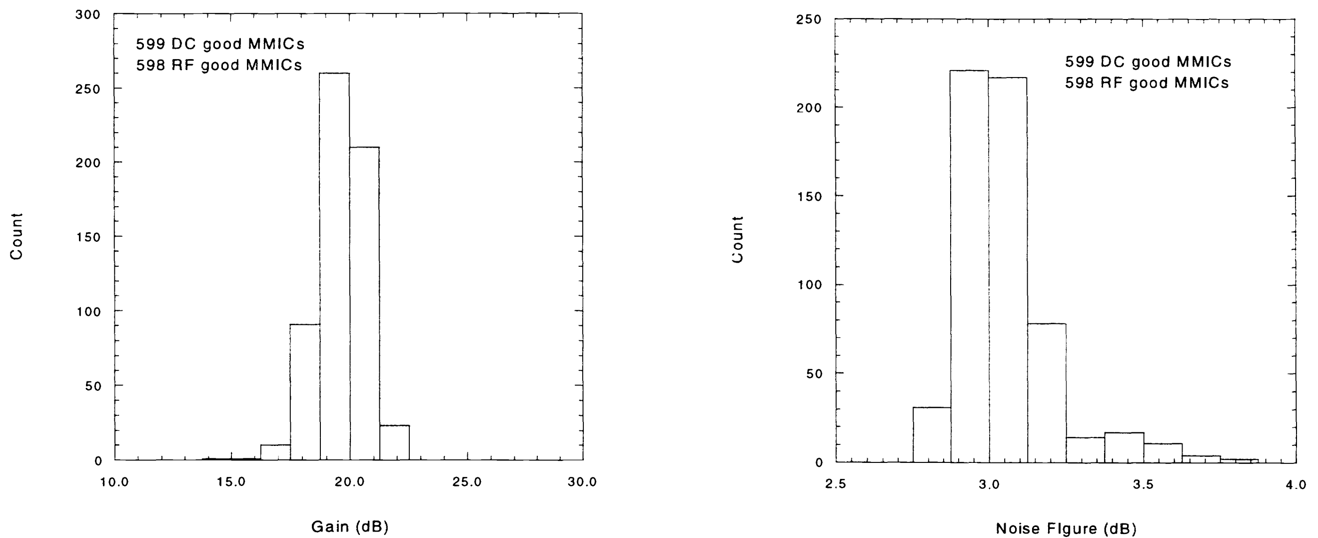

Figure 9. Histograms showing process consistency for gain (left) and noise figure (right) for the 86LN1A amplifiers at 85 GHz from wafer # 1669.

Downloaded From: https://www.spiedigitallibrary.org/conference-proceedings-of-spie on 7/31/2018
Terms of Use: https://www.spiedigitallibrary.org/terms-of-use

		Gain (dB)	NF (dB)			Gain (dB)	NF (dB)
Wafer # 1669							
70LN3A	Average	23.794	3.303	86LN1A	Average	19.663	3.052
DC Yield: 68%	Std. Dev.	0.839	0.189	DC Yield: 70%	Std. Dev.	0.945	0.160
Wafer # 1673							
70LN3A	Average	24.254	3.098	86LN1A	Average	19.925	2.949
DC Yield: 66%	Std. Dev.	0.617	0.159	DC Yield: 69%	Std. Dev.	0.500	0.087
Wafer # 1674							
70LN3A	Average	24.374	3.201	86LN1A	Average	21.965	2.932
DC Yield: 70%	Std. Dev.	0.787	0.133	DC Yield: 70%	Std. Dev.	0.730	0.163
Wafer # 1683							
70LN3A	Average	24.021	3.137	86LN1A	Average	21.399	2.944
DC Yield: 79%	Std. Dev.	0.868	0.166	DC Yield: 77%	Std. Dev.	0.754	0.177
Wafer # 1684							
70LN3A	Average	23.615	3.284	86LN1A	Average	21.846	3.058
DC Yield: 81%	Std. Dev.	0.682	0.127	DC Yield: 58%	Std. Dev.	0.805	0.160
Wafer # 1851							
70LN3A	Average	24.486	2.954	86LN1A	Average	22.118	2.747
DC Yield: 53%	Std. Dev.	0.577	0.138	DC Yield: 62%	Std. Dev.	0.619	0.134

Table 1. Statistical RF performance of production W-band LNAs at 85 GHz.

5. SUMMARY

We have shown state-of-the-art W-band LNA performance using a high yield, highly consistent InP-based HEMT MMIC process. With the availability of large numbers of LNAs with similar characteristics, many mm-wave array applications are realizable. The advanced InP-based HEMT technology used has demonstrated a twofold reduction in equivalent input noise temperature, T_e at room temperature. Nearly 7,000 LNAs were produced in the six wafer lot with highly consistent performance.

ACKNOWLEDGEMENTS

This work was supported by Trex Enterprises, San Diego, California through contract with the U. S. Army Research Laboratory (DAAL01-94-C-0100). The authors wish to thank Joe Galliano and Trex Enterprises for their kind permission to share this technical information.

REFERENCES

1. G. I. Ng et al., "A Fully Passivated Ultra Low Noise W-Band Monolithic InGaAs/InAlAs/InP HEMT Amplifier," *1995 IEEE Microwave and Millimeter-Wave Monolithic Circuits Symp. Dig.*, pp. 63-66.
2. U. K. Mishra and J. B. Shealy, "InP-Based HEMTs: Status and Potential," *Proc. 6th Int. Conf. Indium Phosphide and Related Materials*, 1994, pp.14-17.
3. P. M. Smith et al., "W-band High Efficiency InP-Based Power HEMT with 600 GHz f_{max}," *IEEE Microwave Guided Wave Lett.*, vol.5, no.7, July 1995, pp. 230-232.
4. H. Wang et al., "A 155-GHz Monolithic InP-Based HEMT Amplifier," *1997 IEEE MTT-S Int. Microwave Symp. Dig.*, pp. 1275-1278.
5. C. Pobanz et al., "A High-Gain Monolithic D-band InP HEMT Amplifier," *1998 IEEE Gallium Arsenide Integrated Circuit Symp. Dig.*, pp. 41-44.
6. M. W. Pospieszalski, "Modeling of Noise Parameters of MESFETs and MODFETs and their Frequency and Temperature Dependence," *1989 IEEE MTT-S International Microwave Symp. Dig.*, pp. 385-388.

Downloaded From: https://www.spiedigitallibrary.org/conference-proceedings-of-spie on 7/31/2018
Terms of Use: https://www.spiedigitallibrary.org/terms-of-use